


Effect of solvent gradient inside the entropic trap on polymer migrationDibyajyoti Mohanta^{*} and Debaprasad Giri[†]
*Department of Physics, IIT (BHU), Varanasi 221005, India*Sanjay Kumar[‡]
Department of Physics, Institute of Science, BHU, Varanasi 221005, India (Received 29 July 2021; accepted 8 February 2022; published 24 February 2022)

By employing the exact enumeration technique on the lattice model of a polymer, we study the migration of the polymer chain across an entropic trap in a quasiequilibrium condition and explore the effect of solvent gradient present in the entropic trap which acts both parallel and perpendicular to the direction of migration. The Fokker-Planck formalism utilizes the free energy landscape of a polymer chain across the channel in the presence of the entropic trap to calculate the migration time. It is revealed that the migration is fast when the solvent gradient acts along the migration axis (i.e., x axis) inside the channel in comparison to the channel having the entropic trap. We report here for the first time that the entropic trap makes the migration faster at a certain value of solvent gradient. We also study the effect of transverse solvent gradient (along the y axis) inside the trap and investigate the structural changes of the polymer during migration through the channel. We observe the nonmonotonic dependence of migration time on the solvent gradient.

DOI: [10.1103/PhysRevE.105.024135](https://doi.org/10.1103/PhysRevE.105.024135)**I. INTRODUCTION**

Length scales of living cells and organelles and their operations in a confined environment motivate biologists and physicists to study biopolymers in finite length systems [1–3]. The advent of single-molecule manipulation techniques, such as magnetic tweezers, optical tweezers, atomic force microscopy (AFM), etc. lead to new insights in polymer translocation processes in a confined geometry [4–6]. For example, a nanopore that connects a viral capsid to a cell membrane allows viral DNA to translocate through it, and finally be injected into the cell [7,8]. Also, the movement of proteins through the cell membrane, RNA transport through nuclear pore complexes, and transport of polymers across a gel in electrophoresis are among the other potential applications involved in migration processes [9,10].

Single-molecule studies revealed that the migration process is delayed due to microfluidic channels which enhances the readability of the sequence [11,12]. The migration processes of polymers are often hindered for various reasons. One can classify them into two broad categories: (i) geometrical trapping arising due to confinement effects and (ii) field mediated migration. In geometrical trapping, biopolymers face free energy barriers due to the nanopore geometry or the entropic trap arrays during migration [13]. The basic concept is that whenever the dimension of confinement is smaller than the length of the polymer, the number of accessible configurations of the polymer is considerably reduced. This explains the formation of free energy barriers and the reduction in

associated configurational entropy [14,15]. In contrast, field induced polymer migrations are mostly dominated by the applied electric field or chemical gradient across the pore [16,17]. Wong and Muthukumar [18] experimentally observed that the translocation process of RNA inside an α -hemolysin protein pore was affected by the pH -gradient across the pore. The presence of pH gradient (or solvent gradient) arises due to the protonation of charged amino acid residues inside the pore. Buyukdagli [19] showed that inclusion of a pressure gradient in a driven polymer migration results in extended migration time. Tsutsui *et al.* [20] experimentally observed that a transverse electric field in a silicon dioxide nanochannel slowed down the biopolymer migration velocity. Lam *et al.* [21] proposed the use of ultrathin nanoporous silicon nitride membranes as entropic traps to confine polymers for long times within a nanochannel.

Migrations induced by chemical gradients along the migration axis often form globules on the poor solvent side and these globules acts as ratchets to attract more segments from the good solvent side [22,23]. The manipulation of the solvent quality in the presence of a patchy channel makes the translocation fast, which helps in drug delivery through dendritic carrier molecules [24]. A noteworthy and complex phenomenon happens when a solvent gradient or dielectric constant gradient is introduced in transverse fashion within the nanopore such that the solvent quality differs along the perpendicular direction of the migration axis. Ajdari and Prost [25] theoretically predicted that DNA confined in a geometrical trap with a transverse gradient field in addition to a uniform field along the flow may confine DNA within the trap. Regtmeier *et al.* [26] experimentally verified the findings of Ajdari and Prost [25] by taking an inhomogeneous field along with a constant field, which results in slow migration. This

^{*}dibyajyoti@rs.phy15.@itbhu.ac.in[†]dgiri.app@iitbhu.ac.in[‡]ksanjay@bhu.ac.in

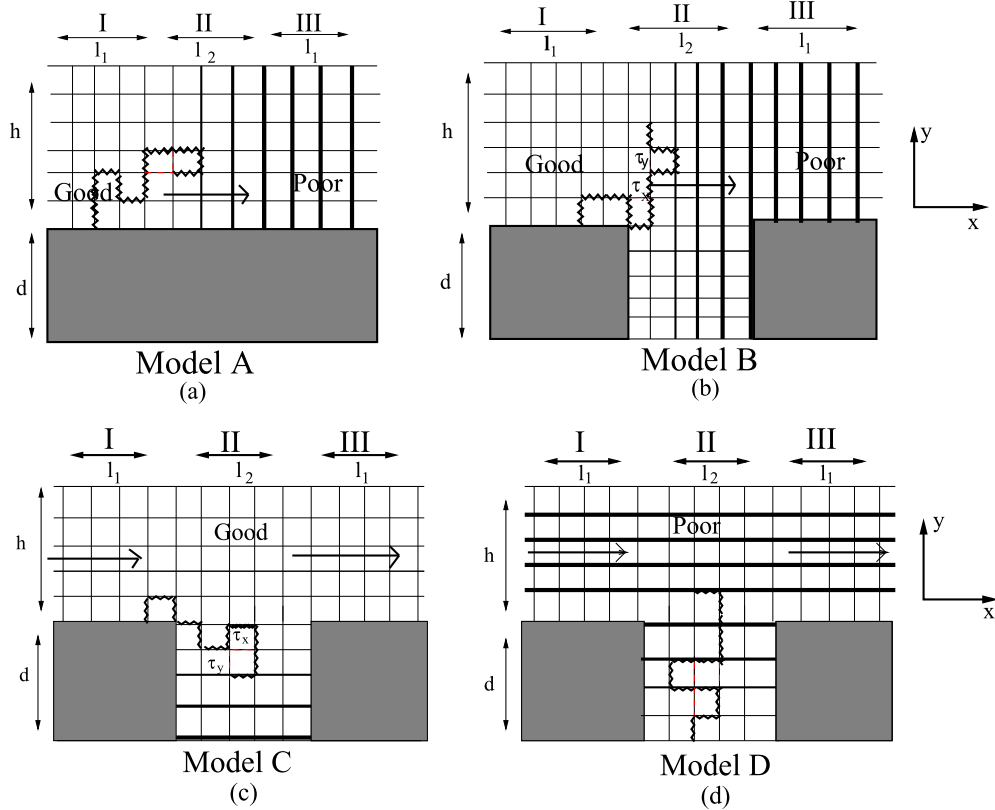


FIG. 1. Schematic representations of polymer chain migration through an inhomogeneous channel. The channel has three different regions (I, II, and III) of a certain length ($l_1 = 14$, $l_2 = 10$ lattice units), width ($h = 12$ lattice units) and different solvent quality (good, poor, and solvent gradient): (a) Model A: Channel without entropic trap and solvent interaction gradient (in region II) is along the x direction. (b) Model B: Channel with entropic trap of depth $d = 10$ lattice units and solvent interaction gradient (in region II) is along the x direction. The red dashed line shows the nonbonded nearest neighbor pairs (within the region where solvent gradient is present) along x and y directions, and corresponding Boltzmann weights are represented by τ_x and τ_y . (c) Model C is the same as model B, but the solvent interaction gradient inside an entropic trap (region II) acts along the transverse direction (y axis). (d) Model D is the same as the model C, but the solvent interaction gradient has the reverse sign compared to model C.

helps in understanding DNA separation with good selectivity, which is essential for human genome mapping [25].

A chemical gradient inside the nanopore channel in either the horizontal or transverse direction may have different effects on polymer migration and be involved in different biological implications [13,18,25,26]. Motivated by this, we study the polymer migration through an entropic trap in the presence of the gradient in the horizontal as well as transverse directions. In order to model the horizontal and transverse gradient fields, we consider a varying nonbonded nearest neighbor attraction among the monomers (ϵ). Here, we focus mostly on the issues where the effective change in nonbonded nearest neighbor interaction (gradient field) hinders the uniform migration in the framework of quasiequilibrium statistical mechanics.

A large number of theoretical and simulation studies describing the complexity of the migration process rely on the quasiequilibrium approach [27–31]. In theoretical quasistatic migration studies, where the time taken by each successful migration step is greater than the relaxation time of the polymer, one can use the Fokker-Planck equation [32–35] to calculate the migration time. In such an approach the migration is usually unidirectional. It is further assumed that

the movement of the polymer is slow enough so that the diffusion coefficient of the polymer can be considered as a constant parameter throughout the process [34]. The aim of this paper is to illustrate the role of the solvent interaction gradient ($\Delta\epsilon$) in the presence of an entropic trap on the migration.

The paper is organized as follows. In Sec. II, we briefly describe the model and method used to study the migration of polymer through the channel in the presence of an entropic trap. In Sec. III, we obtain the free-energy landscape and calculate the associated migration time. We have calculated the x and y components of the radius of gyration to study the configurational properties of the polymer during the migration in Sec. IV. A brief discussion and future perspective of the present work are found in Sec. V.

II. MODEL AND METHOD

In this study, we model a polymer chain migrating through a nonuniform channel with and without an entropic trap. The solvent interaction gradients varying along x and y directions are shown in Figs. 1(a)–1(b) and 1(c)–1(d) respectively. First, we model the polymer chain as a self-attracting–self-avoiding

walk (SASAW) on a square lattice [36–40]. Monomers are sites occupied by the polymers, and interactions are among nonbonded nearest neighbor monomers. The thermodynamic properties of a polymer chain in a solvent of uniform quality are expressed in the form of averages of the physical observables derived from the partition function. The canonical partition function for the polymer chain of length N in a homogeneous system can be written as

$$Z = \sum_{\text{all walks}} \tau^{N_p}. \quad (1)$$

The summation is over all the possible walks and $\tau = \exp(-\beta\epsilon)$ is the Boltzmann weight corresponding to the nonbonded nearest neighbor. Here, $\beta = \frac{1}{K_B T}$, where K_B is the Boltzmann constant and T is the temperature. N_p is the number of nearest neighbor pairs, where each pair has energy ϵ . In this work, we have taken the chain length $N = 28$. We also set $K_B = 1$ and $-1 \leq \epsilon \leq 0$ from here onward.

In order to study the effect of free energy barriers arising due to inhomogeneity inside the channel, we introduce three different regions (I, II, and III) of different dimensions and solvent quality (good or poor) in the presence (or absence) of an entropic trap as shown in Figs. 1(a)–1(d). For the sake of simplicity, we introduce four different models, namely, models A, B, C, and D depending on the solvent gradient (along the channel or perpendicular to the channel) and entropic trap [Figs. 1(a)–1(d)]. Here, we study migration properties in the absence [Fig. 1(a): model A] and in the presence [Fig. 1(b): model B] of an entropic trap having the solvent interaction gradient along x axis while the other parameters remain constant.

In models A and B [Figs. 1(a) and 1(b)], regions I and III have the dimensions length (l_1) and width (h) of 14 and 12 lattice units, respectively. The middle region II of model A has dimensions length (l_2) and width (h) of 10 and 12 lattice units, respectively. Model B has an entropic trap of dimension length (l_2) 10 and depth (d) 10 lattice units. The interest here is to study the migration of a polymer chain from region I to region III and delineate the role of an entropic trap on the free energy barriers and the migration time. Here, we introduce a solvent interaction gradient ($\Delta\epsilon = \frac{\epsilon}{l_2}$) along the channel direction (x axis). The strength of the interaction associated with nearest neighbor pairs in this region (indicated by thin and thick lines in Fig. 1) may be defined as $\epsilon(l_2^i) = l_2^i \Delta\epsilon(l_2)$, where $i = 1, 2, 3, \dots, 10$. It may be noted here that the first layer of region II has the value of $\epsilon(l_2^1 = 1) = 0$ (good), whereas the last layer of region II has the value of $\epsilon(l_2^{10} = 10) = -1$ (poor) for $\Delta\epsilon = -0.1$. Region II is the interface between the two regions I and III as the solvent of region III follows the solvent quality of the last layer of region II depending on the value of $\Delta\epsilon$. It is pertinent to mention here that for $\Delta\epsilon = 0.0$ the solvent quality remains good across all regions of the channel in both models A and B. Here, we show that this simple form of solvent gradient captures the essential physics of migration by considering different nearest neighbor interactions arising in the x and y directions [41].

In regions I and III the Boltzmann weight for the nonbonded nearest neighbor interaction is $\tau = \exp(-\beta\epsilon)$. In

region II, the nonbonded nearest neighbor interaction is uniform along the y direction and has weight

$$\tau_y(x) = \exp[-\beta\epsilon(x)]. \quad (2)$$

However, for the nonbonded nearest neighbor involved in between x and $(x \pm 1)$ layers, the Boltzmann weight can be expressed as

$$\tau_x(x) = \exp\left(-\frac{\beta}{2}[\epsilon(x) + \epsilon(x \pm 1)]\right). \quad (3)$$

Model B is similar to model A, except it has an entropic trap ($l_2 = 10$ lattice units and $d = 10$ lattice units) in region II, as shown in Fig. 1(b).

In this work, the canonical partition function of the model systems can be expressed as

$$Z^x = \sum_{(N_{p1}, N_{p3}, N_{p2}^x, N_{p2}^y, x)} C(N_{p1}, N_{p3}, N_{p2}^x, N_{p2}^y, x) \times \tau_x^{N_{p2}^x} \tau_y^{N_{p2}^y} \tau^{N_{p1}} \tau^{N_{p3}}. \quad (4)$$

Where N_{p1} and N_{p3} are the numbers of nonbonded pairs formed in regions I and III respectively. N_{p2}^x and N_{p2}^y are the nonbonded nearest neighbor contacts along x and y directions, respectively, in region II.

The solvent quality inside the channel is good and poor in models C and D [Figs. 1(c) and 1(d)], respectively. However, the solvent gradient interaction is perpendicular to the direction of migration [25,26]. In model C, the solvent gradient interaction decreases with the depth of the entropic trap, whereas in model D it increases with the depth of the entropic trap. This is analogous to the situation where the quality of the solvent is relatively poor (low temperature regime) at the bottom layer of model C. On contrast to model C, the entropic trap of model D has relatively good solvent ($\epsilon = 0$) at the bottom, i.e., the bottom layer is at high temperature. In both models C and model D the gradient ($\Delta\epsilon = \frac{\epsilon}{d}$) is defined in such a way that the nonbonded pair at the bottom layer contributes $-1 < \epsilon < 0$. For these cases, interactions at any layer inside the entropic trap may be defined as $\epsilon(d^i) = \epsilon + d^i \Delta\epsilon$, where $i = 1, 2, 3, \dots, 10$. The value of $\Delta\epsilon$ lies between 0 and -0.1 for model C and 0 to 0.1 for model D.

The nonbonded nearest neighbor interaction inside the entropic trap remains constant along the x direction, and its Boltzmann weight is given by

$$\tau_x(y) = \exp[-\beta\epsilon(y)]. \quad (5)$$

Whereas if any pair occurs between the y th and $(y \pm 1)$ th layers, then we express the Boltzmann weight as

$$\tau_y(y) = \exp\left(-\frac{\beta}{2}[\epsilon(y) + \epsilon(y \pm 1)]\right). \quad (6)$$

In the equilibrium framework of statistical mechanics, it is difficult to study the migration of a polymer chain. However, if the process is slowed in such a way that the system achieves quasistatic equilibrium at a given instant of time, it is possible to study the dynamics of the system by using the Fokker-Planck equation. The basic ingredient of the Fokker-Planck equation is the free energy of the system at any instant of time for a given value of x . For this, we assume that the

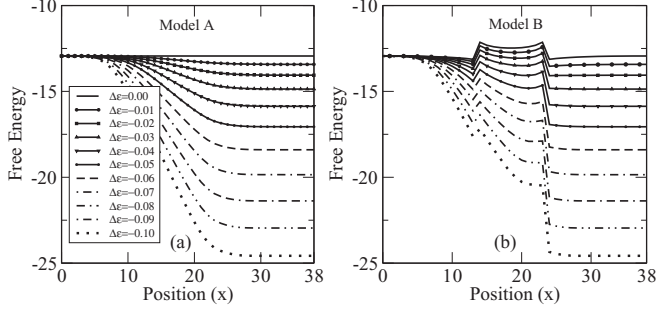


FIG. 2. Variation of the free energy with anchoring coordinate (x) for different solvent interaction gradients ($\Delta\epsilon$): (a) for model A; (b) for model B.

polymer is migrating from region I to region III and the free energy of the system may be obtained by progressively fixing one end of the polymer from $x = 0$ to $x = 38$, whereas other end of the polymer is free to be anywhere inside the channel. All the possible conformations are enumerated at each x coordinate ($x = 0$ to $x = 38$) along the direction of migration. For models B, C, and D, the y coordinate of the polymer is fixed at $y = 0$ whenever the polymer is outside of the trap ($x = 0$ to $x = 13$ and $x = 24$ to $x = 38$). When the polymer is migrating through the entropic trap ($x = 14$ to $x = 23$), the y coordinate is fixed at the bottom ($y = -10$). We used the exact enumeration technique [36] to calculate the partition function for a given value x by using the following equation:

$$Z^x = \sum_{(N_{p1}, N_{p2}^x, N_{p2}^y)} C(N_{p1}, N_{p2}^x, N_{p2}^y, x) \tau_x^{N_{p2}^x} \tau_y^{N_{p2}^y} \tau^{N_{p1}}, \quad (7)$$

where N_{p2}^x and N_{p2}^y are the numbers of nearest neighbor contacts along the x direction and y directions, respectively, inside the entropic trap. $C(N_{p1}, N_{p2}^x, N_{p2}^y, x)$ is the number of distinct configurations having N_{p1} contacts in the channel and $N_{p2} (= N_{p2}^x + N_{p2}^y)$ contacts in the entropic trap. The free energy of the system for a given value of x is given by

$$F^x = -T \log(Z^x). \quad (8)$$

III. FREE ENERGY LANDSCAPE

The migration process may be understood if one has complete information of the free energy associated with each region of the channel. In order to have a better understanding the effect of the entropic confinement on the migration process, we systematically calculate the free energy of the system as a function of x , where one end of the chain is anchored. It may be noted that in both models A and B, region I has a good solvent ($\epsilon = 0$) and the gradient acts along the x direction, and they differ only in terms of the entropic trap. For model A, when $\Delta\epsilon = 0.0$, the free energy remains constant throughout the channel [Fig. 2(a)]. This implies that monomer-monomer attractions remain absent ($\epsilon = 0$) throughout the channel for regions I, II, and III. Now we systematically vary the nearest neighbor attraction among the monomers at the interval of 0.1 in the region III. This gives rise to the solvent interaction gradient in region II. As $\Delta\epsilon$ decreases, one end of region II (near the poor side) becomes poorer compared to the side

which is close to the good solvent. As a result, the polymer prefers to move towards region II as free energy decreases and approaches the free energy of region III. The migration seen in model A closely resembles the characteristics of voltage driven translocation [42–44]. The presence of the entropic trap (model B) shows some interesting behavior which can be seen in Fig. 2(b). The appearance of the free energy barrier for low $\Delta\epsilon$ and the change in slope in the free energy curve at the interfaces of regions I and II and regions II and III are some notable observations which may influence the migration behavior inside the channel. For $\Delta\epsilon = 0.0$, where the solvent quality throughout the channel remains good, the appearance of the free energy barrier at the interfaces of regions I and II and regions II and III is solely due to the entropic trap. As $\Delta\epsilon$ decreases, the solvent quality of region II becomes more poorer compared to region I. The decrease in $\Delta\epsilon$ makes the migration process easier. The free energy decreases gradually from region I to region II and approaches the free energy of region III.

For both models the gradient enhances the migration process; however, the entropic trap reduces the process in comparison to model A. To substantiate this, one can calculate the average time involved in migration between the initial (region I) and final (region III) stages. Since the free energy of the polymeric system is known, one can employ the Fokker-Planck formalism to obtain the migration time from region I to region III. The governing equation is

$$\frac{\partial}{\partial t} p(x, t) = L(x)p(x, t), \quad (9)$$

where $p(x, t)$ is the probability distribution. $L(x)$ is the Fokker-Planck operator described by

$$L(x) = \frac{1}{b^2} \frac{\partial}{\partial x} D(x) \exp[-F(x)] \frac{\partial}{\partial x} \exp[F(x)], \quad (10)$$

where $F(x)$ is the free energy of the polymer. $D(x)$ is the diffusion coefficient and b is the bond length. Following the method developed in Ref. [29], we set $D(x) = 1$. Since the present study is confined on the lattice, we assigned the bond length to be unity and the migration time has been expressed in the following discrete form:

$$\tau_{(x=0;x=38)} = \sum_{x'=0,1,2,\dots,38} \Delta x' \exp[F(x')] \times \sum_{x''=0}^{x'} \Delta x'' \exp[-F(x'')]. \quad (11)$$

Here, the first summation adds the contribution of free energies from $x' = 0, 1, 2, \dots, 38$ to $x' = 38$, whereas the second summation sums up the free energy contributions from $x'' = 0$ to x' . Here, we have taken $\Delta x'' = \Delta x' = 1$ in lattice units.

The migration times required to reach region III from region I for models A and B are shown in Fig. 3 as a function of $\Delta\epsilon$. It is evident from the plots that for $\Delta\epsilon = 0$ the free energy barrier arising due to the entropic trap (model B) offers slow migration in comparison to model A. This is in accordance with experimental observation where the entropic trap slows down the migration of biopolymers through microchannels [13,21,45]. The decrease in $\Delta\epsilon$ corresponds to the reduction in

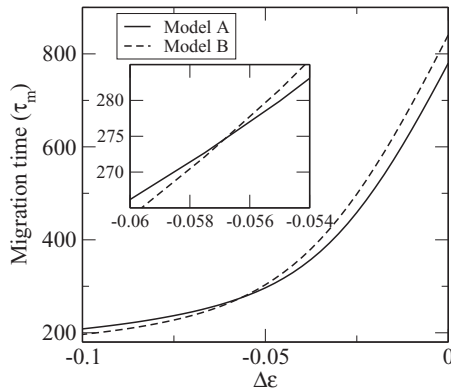


FIG. 3. Variation of the migration time (τ_m) with $\Delta\epsilon$ for model A and model B. In the inset we show the region where migration time for model B exceeds that of model A.

the free energy which in turn expedites the migration towards region III. One of the interesting observations is that for both models the migration time (τ_m) decreases; however, around $\Delta\epsilon \sim -0.057$, the migration time for model A exceeds that of model B. This may be explained on the basis of subtle competition between the increase in entropy and the solvent interaction gradient. We may substantiate this result with the argument that due to the entropic trap polymer exposure in the gradient (region II) also increases, which eventually drives the polymer towards region III. As a result one observes lower migration time for model B compared to model A for $\Delta\epsilon < -0.057$. As the anchor sites move away from the entropic trap, the migration time approaches monotonically towards that of model A.

It would be interesting to study the effect of transverse gradient which may be present in the entropic trap. In this context two situations may arise: (i) the channel has a good solvent ($\epsilon = 0$), while the entropic trap contains a relatively poor solvent (model C); (ii) the channel contains a poor solvent ($\epsilon = -1$), whereas the entropic trap has a relatively good solvent (model D). In both cases we assigned the transverse nearest neighbor interaction gradient by substituting $-0.1 \leq \Delta\epsilon \leq 0$ for model C and $0 \leq \Delta\epsilon \leq 0.1$ for model D. As a result the nearest neighbor attraction at the bottom layer of the entropic trap will have the value $-1 \leq \epsilon \leq 0$ for model C and $-1 \leq \epsilon \leq 0$ for model D. This ensures a decrease in solvent gradient with the depth of the trap for model C and an increase in solvent gradient with the depth of the entropic trap for model D. This is analogous to the situation where the bottom layer of the entropic trap is at lower temperature compared to the temperature of the channel. In contrast to model C, the channel of model D has a lower temperature compared to the entropic trap. Our model system is analogous to earlier studies [25,26] where a transverse field is used inside the entropic trap.

Figure 4(a) shows the free energy landscape (for model C) as a function of x where one end of the polymer is anchored. For $\Delta\epsilon = 0.0$, the solvent quality remains uniform in the entropic trap as well as across the channel. One can observe the barrier in the free energy landscape which arises due to the confinement imposed by the entropic trap. Because of the

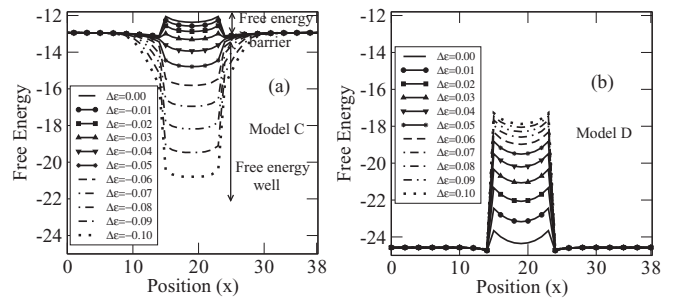


FIG. 4. The free energy landscape for different values of $\Delta\epsilon$: (a) for model C; (b) for model D. The arrows shown in Fig. (a) indicate the free energy barrier and free energy well.

entropic trap, there is a significant decrease in the configurational entropy of the polymer chain which gives rise to the barrier. As $\Delta\epsilon$ decreases, the solvent quality of the trap turns out to be poorer compare to the solvent quality of the channel. As a result, there is a decrease in the free energy arising due to the solvent gradient which overcomes the entropic barrier. A further decrease in $\Delta\epsilon$ transforms the free energy barrier to a well. It would be interesting to note that both the free energy barrier and well hinder the polymer movement across the channel. The time involved in the migration process from region I to region III is minimum around $\Delta\epsilon \sim -0.03$. This corresponds to a net balance between entropic barrier and solvent interaction gradient to the free energy.

Since the channel in model D contains poor solvent all across the channel for $\Delta\epsilon = 0$, one can see a free energy barrier similar to that seen in model C. However, as solvent quality in the entropic trap becomes good ($\Delta\epsilon > 0$) the barrier height increases across the trap. Unlike model C, here the barrier height always increases. As a result one expects larger migration time. The migration time for models C and D is shown in Fig. 5. Model C shows nonmonotonic dependence on $\Delta\epsilon$ [Fig. 5(a)]. When $\Delta\epsilon$ decreases ($\Delta\epsilon < 0$), a free energy well is formed across the trap. Here, the polymer acquires the configuration of the globule state and remains confined in the trap. As a result the time required for the migration is found to be large. As $\Delta\epsilon$ increases, the solvent quality of the trap tends towards the good solvent and thus the globule gets destabilized due to increase in configurational entropy. In contrast to model C, model D shows the migration time monotonically increasing with $\Delta\epsilon$ [Fig. 5(b)]. This may be

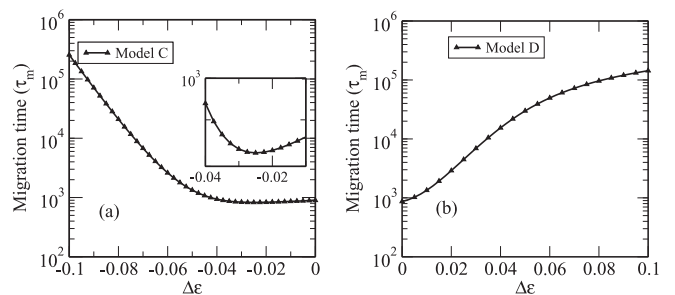


FIG. 5. Variation of the migration time with $\Delta\epsilon$: (a) for model C; (b) for model D. The inset of (a) shows the minimum of migration time for model C.

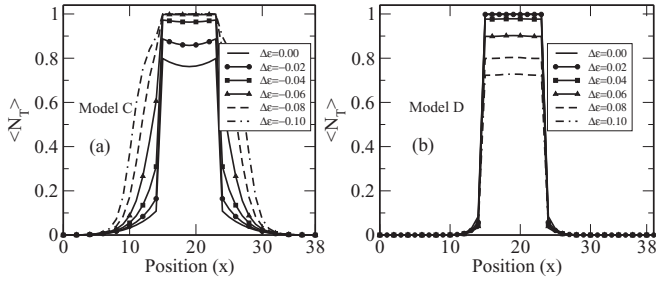


FIG. 6. The average number of monomers inside the trap ($\langle N_T \rangle$) for different $\Delta\epsilon$: (a) for model C; (b) for model D.

understood by making the solvent quality good inside the trap and leads to the conformation of the polymer chain in the swollen state. As $\Delta\epsilon$ increases, the trap becomes more repulsive and the free energy barrier increases. An increase in barrier height further enhances the migration time.

It is interesting to note that the migration times are nearly equal for $\Delta\epsilon = 0$ for both models C and D. This indicates that for the good solvent channel (model C with $\Delta\epsilon = 0$) and poor solvent channel (model D with $\Delta\epsilon = 0$), the polymer takes almost the same time. This is because the appearance of the free energy barrier at $\Delta\epsilon = 0$ is solely entropic and hence the same for both models. The presence of gradient ($\Delta\epsilon > 0$) inside the entropic trap makes the migration process slow.

IV. CONFIGURATIONAL PROPERTIES OF POLYMER DURING MIGRATION

It would be interesting to investigate how the configurational properties of the polymer change due to the solvent interaction gradient in the entropic trap. For this, we first calculate the average number of monomers ($\langle N_T \rangle$) inside the trap as a function of x . It may be pointed out here that the trap coordinates lie within $13 < x < 24$. Fig. 6(a) shows the fraction of monomers inside the trap (model C) as a function of x , which is almost negligible when the anchored sites are far away from the trap. As the anchor site approaches the trap, $\langle N_T \rangle$ starts increasing. As $\Delta\epsilon$ decreases, a part of the polymer favors being inside the trap and tends to acquire the globule state. This behavior is also evident from the free energy curve [Fig. 4(a)] where the free energy decreases before the anchor site reaches near the trap. This corresponds to a fraction of segments remaining in the swollen state due to the anchor site; however, the remaining segment inside the trap forms the globule. Figure 6(b) shows the variation of $\langle N_T \rangle$ with x for model D. Here, we focus on when the polymer is mostly confined in region II, i.e., inside the trap. Here, the polymer remains in the globule state around the anchor sites (outside the trap) and does not experience any effect of solvent in the trap. When the anchor site is forced to be inside the trap, a part of the polymer segment remains in the swollen state (inside the trap) whereas the remaining part will be outside the trap, but in the globule state. When $\Delta\epsilon \rightarrow 0$ (i.e., solvent in the channel and inside the trap remain the same), it acquires the globule state inside the trap.

The variations in shape of the polymer in terms of the radius of gyration ($\langle R_g^2 \rangle$) as a function of anchoring coordinates

(x) for models C and D are shown in Figs. 7(a) and 7(d), respectively. For both models, we observe slight increase in $\langle R_g^2 \rangle$ near the edge of the trap compared to the middle of the trap. This is because near the edge the polymer has the option to spread along the y -direction and that maximizes the monomer density at the edge. As one moves towards the center of the trap, polymer can spread in all directions and thus $\langle R_g^2 \rangle$ decreases for model C and increases for model D [Figs. 7(a) and 7(d)]. $\Delta\epsilon \approx -0.03$, which corresponds to the minimum migration time, also shows the least variation in $\langle R_g^2 \rangle$ all across the channel for model C. As $\Delta\epsilon$ decreases, the quality of the solvent becomes poorer for model C and hence $\langle R_g^2 \rangle$ decreases. As a result the migration time also increases. On the other hand, in model D the solvent quality tends towards a good solvent with $\Delta\epsilon$, and thus $\langle R_g^2 \rangle$ tends to its swollen state value.

Since the microscopic variation in shape arising due to confinement is not quite apparent from Figs. 7(a) and 7(d), we study the variation of polymer shape in terms of the x and y components of the radius of gyration as a function of x . The variations in $\langle R_{gx}^2 \rangle$ and $\langle R_{gy}^2 \rangle$ are shown in Figs. 7(b), 7(c) and Figs. 7(e), 7(f) for models C and D respectively. One can notice from the plots that the entropic trap in presence of the solvent interaction gradient affects $\langle R_{gy}^2 \rangle$, whereas $\langle R_{gx}^2 \rangle$ remains almost the same. It may be noted that the model C has relatively poor solvent inside the trap, and thus there is a natural tendency to minimize its free energy, even if the anchor site is outside the trap. This may be seen in the variation of both $\langle R_{gx}^2 \rangle$ and $\langle R_{gy}^2 \rangle$, when the anchor sites are outside the trap. The most interesting observation is the increase in $\langle R_{gy}^2 \rangle$ as a function of x and then sudden decrease for $\Delta\epsilon < -0.03$. This may be understood as the bottom surface of the trap having a poor solvent (lower temperature) and thus a major fraction of the polymer chain prefers to stay in the globule state, whereas its anchor site is outside the trap. As a result, the polymer is forced to acquire the conformation along the side of the trap (y axis) and thus $\langle R_{gy}^2 \rangle$ increases. In contrast to model C, model D shows [Figs. 7(c) and 7(f)] gradual decrease in $\langle R_{gx}^2 \rangle$ and increase in $\langle R_{gy}^2 \rangle$ as a function of x inside the trap for a given chain length. When $\Delta\epsilon = 0$, the solvent all across the channel is poor and the polymer remains in the globule state inside the trap, as well as outside the trap. This is evident from Figs. 7(c) and 7(f) where both components of $\langle R_g^2 \rangle$ remain almost the same. As $\Delta\epsilon$ increases, the solvent inside the trap becomes good and the y component of $\langle R_g^2 \rangle$ increases. In this situation, the polymer acquires a “mushroom” shape in such a way that the major fraction of the polymer prefers to be outside the trap in the globule form [46]. This in turn reduces $\langle R_{gx}^2 \rangle$, which approaches 1 as shown in inset of Fig. 7(e)

V. CONCLUSION

In this work, we have studied the effects of solvent interaction gradient inside an entropic trap on the migration of a polymer. Employing the exact enumeration technique and by varying the anchoring sites of one end of the anchored polymer, we have studied the migration of the polymer from one side (region I) to the other (region III) by assuming that

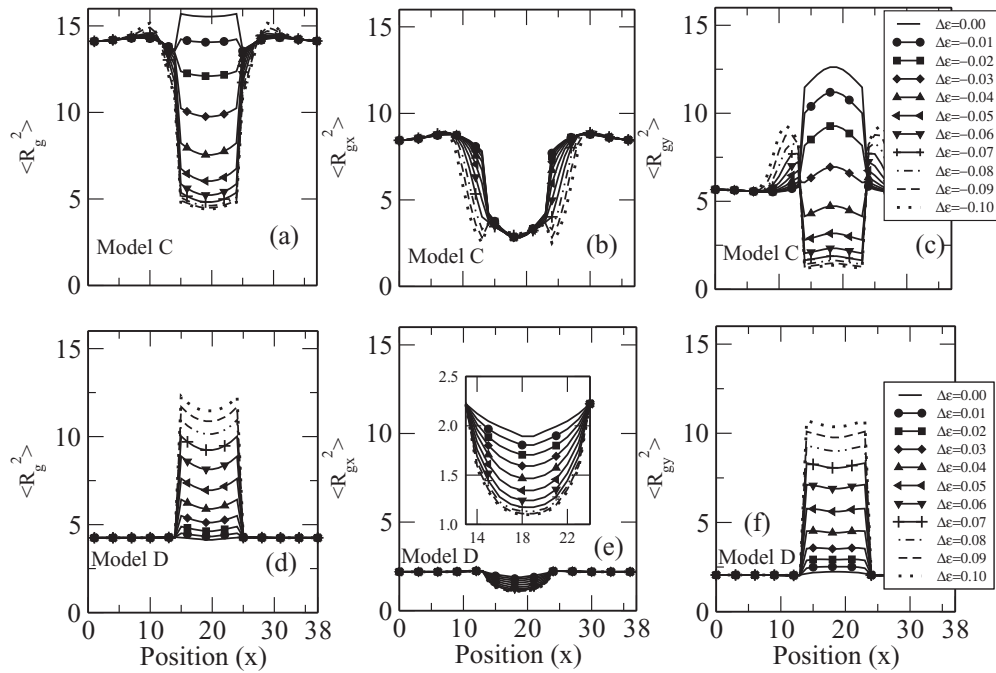


FIG. 7. (a) Variation of the radius of gyration ($\langle R_g^2 \rangle$) with x for different $\Delta\epsilon$ for model C. (b) Variation of the x component of the radius of gyration ($\langle R_{gx}^2 \rangle$) with x for different $\Delta\epsilon$ for model C. (c) Variation of the y component of the radius of gyration ($\langle R_{gy}^2 \rangle$) with x for different $\Delta\epsilon$ for model C. (d)–(f) Same as (a)–(c) but for model D.

the system remains in a quasistatic equilibrium condition. We have considered the solvent interaction gradient both parallel and perpendicular to the migration direction in region II. The free energy landscapes of model A (without entropic trap) and model B (with entropic trap) differ significantly and show the influence of the entropic trap. Using the Fokker-Planck equation we obtain the migration time, which shows that as $\Delta\epsilon$ decreases the migration time decreases. The exact calculation based on the short chain revealed that, for a certain value of $\Delta\epsilon$, the entropic trap may reduce the migration time.

In contrast to models A and B where the gradient is taken along the x axis, we have explored the effect of transverse gradient (y axis) in the presence of an entropic trap in models C and D. We have considered two possibilities: the channel has a good solvent (high temperature) and the solvent confined in an entropic trap is poor (low temperature), and vice versa. We have imposed a linear solvent interaction gradient and studied the migration behavior of the polymer chain from region I to region III in the presence of an entropic trap. In this case, the migration time shows a nonmonotonic behavior as a function of solvent interaction gradient for model C, whereas it shows a monotonic increase in the case of model D. At $\Delta\epsilon \approx -0.023$, the free energy barrier/well vanishes and at this value the migration time is found to be the minimum. Our exact calculations reveal that with increasing length or decreasing solvent quality inside trap the nonmonotonic trend in migration time becomes more apparent. A future experiment will be able to

observe it for a longer chain. Interestingly, model D has a free energy barrier which increases with $\Delta\epsilon$ and hence migration time increases monotonically. It is pertinent to mention here that the applicability of the Fokker-Planck formalism depends on the condition where migration time at each step is greater than the relaxation time of the polymer (slow migration) [29,30,39], which is the case studied here.

We have also explored the variation in the shape of the polymer inside the trap for models C and D. We observed that the entropic trap has significant impact on the y component of $\langle R_g^2 \rangle$, whereas the x component remains almost the same. Our studies suggest that the entropic trap having good solvent (model D) may give rise to a “mushroom” type shape of polymer, which has potential application for the formation of micelles.

ACKNOWLEDGMENTS

Financial assistance from the SERB, India, DST, India, UGC, India, SPARC scheme of MoE, and IoE, MoE, India is gratefully acknowledged. The support and the resources provided by the PARAM Shivay Facility under the National Supercomputing Mission, Government of India at IIT (BHU), Varanasi are gratefully acknowledged. We also acknowledge the computing facility of the Department of Physics, IIT (BHU) and BHU, Varanasi developed under the DST-FIST scheme of DST, New Delhi.

- [1] T. Cremer and M. Cremer, *Cold Spring Harbor Perspect. Biol.* **2**, a003889 (2010).
 [2] S. Jun and A. Wright, *Nat. Rev. Microbiol.* **8**, 600 (2010).

- [3] E. Werner, M. Reiter-Schad, T. Ambjörnsson, and B. Mehlig, *Phys. Rev. E* **91**, 060702(R) (2015); P. K. Mishra and S. Kumar, *J. Chem. Phys.* **121**, 8642 (2004).

- [4] U. Bockelmann, P. Thomen, B. Essevaz-Roulet, V. Viasnoff, and F. Heslot, *Biophys. J.* **82**, 1537 (2002).
- [5] J. Yan, D. Skoko, and J. F. Marko, *Phys. Rev. E* **70**, 011905 (2004).
- [6] P. Saurabh and S. Mukamel, *J. Chem. Phys.* **140**, 161107 (2014).
- [7] D. Marenduzzo, C. Micheletti, E. Orlandini, and D. W. Sumners, *Proc. Natl. Acad. Sci. USA* **110**, 20081 (2013).
- [8] M. M. Inamdar, W. M. Gelbart, and R. Phillips, *Biophys. J.* **91**, 411 (2006).
- [9] G. Schatz and B. Dobberstein, *Science* **271**, 1519 (1996).
- [10] B. H. Zimm and S. D. Levene, *Q. Rev. Biophys.* **25**, 171 (1992).
- [11] P. Y. Lee, J. Costumbrado, C.-Y. Hsu, and Y. H. Kim, *J. Visualized Exp.* **62**, E3923 (2012).
- [12] B. Luan, G. Stolovitzky, and G. Martyna, *Nanoscale* **4**, 1068 (2012).
- [13] M. Wanunu, *Phys. Life Rev.* **9**, 125 (2012).
- [14] J. M. Polson and D. R. Heckbert, *Phys. Rev. E* **100**, 012504 (2019).
- [15] A. Cacciuto and E. Luijten, *Phys. Rev. Lett.* **96**, 238104 (2006).
- [16] S. Kwon and B. J. Sung, *J. Chem. Phys.* **149**, 244907 (2018).
- [17] K. Luo, I. Huopaniemi, T. Ala-Nissila, and S.-C. Ying, *J. Chem. Phys.* **124**, 114704 (2006).
- [18] C. T. A. Wong and M. Muthukumar, *J. Chem. Phys.* **133**, 045101 (2010).
- [19] S. Buyukdagli, *Phys. Rev. E* **97**, 062406 (2018).
- [20] M. Tsutsui, Y. He, M. Furuhashi, S. Rahong, M. Taniguchi, and T. Kawai, *Sci. Rep.* **2**, 394 (2012).
- [21] M. H. Lam, K. Briggs, K. Kastiris, M. Magill, G. R. Madejski, J. L. McGrath, H. W. de Haan, and V. Tabard-Cossa, *ACS Appl. Nano Mater.* **2**, 4773 (2019).
- [22] C. Lorsch, T. Ala-Nissila, and A. Bhattacharya, *Phys. Rev. E* **83**, 011914 (2011).
- [23] P. G. de Gennes and T. A. Witten, *Phys. Today* **33**(6), 51 (1980).
- [24] A. Nikoubashman and C. N. Likos, *J. Chem. Phys.* **133**, 074901 (2010).
- [25] A. Ajdari and J. Prost, *Proc. Natl. Acad. Sci. USA* **88**, 4468 (1991).
- [26] J. Regtmeier, T. T. Duong, R. Eichhorn, D. Anselmetti, and A. Ros, *Anal. Chem.* **79**, 3925 (2007).
- [27] F. Tessier, J. Labrie, and G. W. Slater, *Macromolecules* **35**, 4791 (2002).
- [28] M. Muthukumar, *Polymer Translocation* (CRC, Boca Raton, 2016).
- [29] L. Z. Sun, W.-P. Cao, and M. B. Luo, *J. Chem. Phys.* **131**, 194904 (2009).
- [30] Y. C. Chen, C. Wang, Y. L. Zhou, and M. B. Luo, *J. Chem. Phys.* **130**, 054902 (2009).
- [31] A. Gopinathan and Y. W. Kim, *Phys. Rev. Lett.* **99**, 228106 (2007).
- [32] J. M. Polson and T. R. Dunn, *J. Chem. Phys.* **140**, 184904 (2014).
- [33] J. M. Polson and A. C. M. McCaffrey, *J. Chem. Phys.* **138**, 174902 (2013).
- [34] S. Zhang, C. Wang, L. Z. Sun, C. Y. Li, and M. B. Luo, *J. Chem. Phys.* **139**, 044902 (2013).
- [35] K. Chauhan and S. Kumar, *Phys. Rev. E* **103**, 042501 (2021).
- [36] C. Vanderezande, *Lattice Models of Polymers* (Cambridge University Press, Cambridge, 1998).
- [37] S. Kumar and M. S. Li, *Phys. Rep.* **486**, 1 (2010).
- [38] D. Mohanta, D. Giri, and S. Kumar, *J. Stat. Mech: Theory Exp.* (2019) 043501.
- [39] D. Mohanta, D. Giri, and S. Kumar, *Physica A* **562**, 125379 (2021).
- [40] D. Mohanta, *Physica A* **588**, 126573 (2022).
- [41] S. Nath, D. P. Foster, D. Giri, and S. Kumar, *Phys. Rev. E* **88**, 054601 (2013).
- [42] K. Luo, T. Ala-Nissila, S.-C. Ying, and R. Metzler, *Europhys. Lett.* **88**, 68006 (2009).
- [43] M. Muthukumar and C. Y. Kong, *Proc. Natl. Acad. Sci. USA* **103**, 5273 (2006).
- [44] M. B. Luo, S. Zhang, F. Wu, and L. Z. Sun, *Front. Phys.* **12**, 128301 (2017).
- [45] M. Streek, F. Schmid, T. T. Duong, D. Anselmetti, and A. Ros, *Phys. Rev. E* **71**, 011905 (2005).
- [46] A. Milchev, V. Yamakov, and K. Binder, *Phys. Chem. Chem. Phys.* **1**, 2083 (1999).